

# Uncertainty estimation in spatial interpolation of satellite precipitation with ensemble learning

Georgia Papacharalampous<sup>1,\*</sup>, Hristos Tyralis<sup>2</sup>, Nikolaos Doulamis<sup>3</sup>, Anastasios Doulamis<sup>4</sup>

<sup>1</sup> Department of Topography, School of Rural, Surveying and Geoinformatics Engineering, National Technical University of Athens, Iroon Polytechniou 5, 157 80 Zografou, Greece ([papacharalampous.georgia@gmail.com](mailto:papacharalampous.georgia@gmail.com), [gpapacharalampous@hydro.ntua.gr](mailto:gpapacharalampous@hydro.ntua.gr), <https://orcid.org/0000-0001-5446-954X>)

<sup>2</sup> Department of Topography, School of Rural, Surveying and Geoinformatics Engineering, National Technical University of Athens, Iroon Polytechniou 5, 157 80 Zografou, Greece ([montchrister@gmail.com](mailto:montchrister@gmail.com), [hristos@itia.ntua.gr](mailto:hristos@itia.ntua.gr), <https://orcid.org/0000-0002-8932-4997>)

<sup>3</sup> Department of Topography, School of Rural, Surveying and Geoinformatics Engineering, National Technical University of Athens, Iroon Polytechniou 5, 157 80 Zografou, Greece ([ndoulam@cs.ntua.gr](mailto:ndoulam@cs.ntua.gr), <https://orcid.org/0000-0002-4064-8990>)

<sup>4</sup> Department of Topography, School of Rural, Surveying and Geoinformatics Engineering, National Technical University of Athens, Iroon Polytechniou 5, 157 80 Zografou, Greece ([adoulam@cs.ntua.gr](mailto:adoulam@cs.ntua.gr), <https://orcid.org/0000-0002-0612-5889>)

\* Corresponding author

**Abstract:** Predictions in the form of probability distributions are crucial for decision-making. Quantile regression enables this within spatial interpolation settings for merging remote sensing and gauge precipitation data. However, ensemble learning of quantile regression algorithms remains unexplored in this context. Here, we address this gap by introducing nine quantile-based ensemble learners and applying them to large precipitation datasets. We employed a novel feature engineering strategy, reducing predictors to distance-weighted satellite precipitation at relevant locations, combined with location elevation. Our ensemble learners include six stacking and three simple methods (mean, median, best combiner), combining six individual algorithms: quantile regression (QR), quantile regression forests (QRF), generalized random forests (GRF), gradient boosting machines (GBM), light gradient boosting machines (LightGBM), and quantile regression neural networks (QRNN). These algorithms serve as both base learners and combiners within different stacking methods. We evaluated performance

against QR using quantile scoring functions in a large dataset comprising 15 years of monthly gauge-measured and satellite precipitation in contiguous US (CONUS). Stacking with QR and QRNN yielded the best results across quantile levels of interest (0.025, 0.050, 0.075, 0.100, 0.200, 0.300, 0.400, 0.500, 0.600, 0.700, 0.800, 0.900, 0.925, 0.950, 0.975), surpassing the reference method by 3.91% to 8.95%. This demonstrates the potential of stacking to improve probabilistic predictions in spatial interpolation and beyond.

**Keywords:** ensemble learning; precipitation; predictive uncertainty estimation; probabilistic prediction; spatial interpolation; stacked generalization

## 1. Introduction

Regression applications in spatial interpolation settings include those that merge remote sensing and gauge-measured precipitation data (e.g., Baez-Villanueva et al. 2020; Nguyen et al. 2021; Papacharalampous et al. 2023a). Merging these two data types with machine learning is recognised as an important endeavour in earth observation and geoinformation (Hu et al. 2019; Abdollahipour et al. 2022), as it can lead to spatially dense datasets with larger accuracy than the remote sensing ones. The various remote sensing machine learning regression applications usually issue point predictions through machine learning algorithms such as those described in Hastie et al. (2009), James et al. (2013) and Efron and Hastie (2016). These predictions provide a small amount of information.

The notion of predictive uncertainty estimation in such settings refers to the requirement that precipitation predictions, at every point in space, be given in the form of a probability distribution, instead of a point prediction. Predictive uncertainty estimation is essential because of the large amount of information that it provides to decision makers (Gneiting and Raftery 2007). The literature devoted to methods for predictive uncertainty estimation with machine learning in remote sensing of precipitation is limited with representative examples being demonstrated by Bhuiyan et al. (2018), Zhang et al. (2022), Glawion et al. (2023), Tyralis et al. (2023), Papacharalampous et al. (2024), although machine learning offers several advantages such as improved predictive performance and convenient implementation (Papacharalampous and Tyralis 2022; Tyralis and Papacharalampous 2024).

Our aim is to propose methods for issuing improved probabilistic predictions of precipitation in spatial interpolation settings; in particular, when merging remote sensing

and gauge-measured precipitation data. To this end, we introduce and evaluate several quantile-based ensemble learning methods for predictive uncertainty estimation and demonstrate significant improvement over previous approaches in the same endeavour that are based on individual algorithms (e.g., Bhuiyan et al. 2018; Zhang et al. 2022; Glawion et al. 2023; Tyrallis et al. 2023; Papacharalampous et al. 2024). In particular, none of the cited articles explore ensemble learning for uncertainty estimation, despite its well-established performance improvement over individual algorithms in point prediction applications (Sagi and Rokach 2018; Papacharalampous and Tyrallis 2022; Wang et al. 2023; Tyrallis and Papacharalampous 2024).

Ensemble learning can be made either in simple (equal weight averaging, e.g., Petropoulos and Svetunkov 2020) or complex (e.g., Wolpert 1992) ways. Here, we formulate methods from both these types, because simple averaging can be hard to beat in practice (Smith and Wallis 2009; Lichtendahl et al. 2023). The methods are evaluated in predicting quantiles of the predictive probability distribution at multiple levels, using quantile scoring functions (quantile losses, Gneiting 2011). As minimizing quantile losses is the objective, stacking methods were specifically developed for this purpose. These methods incorporate both linear and non-linear combiners to investigate if the latter's added flexibility impacts the problem at hand.

We apply the methods to a 15-year dataset of monthly gauge-measured and satellite precipitation covering the Contiguous United States (CONUS). Gauge measurements serve as ground truth, while satellite data and gauge elevation play the role of predictor variables. We introduce a new feature engineering method for spatial settings, which halves the number of predictor variables by using distance-weighted satellite data, instead of raw satellite data and distances. This approach eliminates redundant predictor values, particularly distances, potentially improving the performance of non-tree-based algorithms (e.g., Papacharalampous et al. 2023a, b, c, 2024; Tyrallis et al. 2023).

The remaining article is structured in five sections. [Section 2](#) describes the ensemble learning methods and their elements, while [Section 3](#) describes how these methods were applied in this work, including a new feature engineering strategy in spatial interpolation, and the data used for this application. [Section 4](#) presents the results, which are then discussed in view of the pre-existing literature in [Section 5](#). [Section 6](#) concludes the article.

## 2. Ensemble learners

### 2.1 Base learners

Predictive uncertainty estimation can be conducted through a variety of machine learning algorithms (Tyrallis and Papacharalampous 2024). Herein, the interest was in ensemble learners that predict the quantile functional of the probability distribution. For constructing such ensemble learners, we used algorithms from the quantile regression family (see Table 1). Such algorithms either optimize across a training dataset the quantile scoring function (e.g. quantile regression (QR), gradient boosting machines (GBM), light gradient boosting machines (LightGBM) and quantile regression neural networks (QRNN)), a scoring function that is strictly consistent for the quantile functional of the probability distribution (Gneiting 2011), or have been proven optimal for predicting the quantile functional (quantile regression forests (QRF) and generalized random forests (GRF)). The property of strict consistency of quantile scoring functions for the quantile functional incentivizes modellers to report honest evaluations of their quantile predictions; in the sense that when one receives a directive to predict a quantile functional, the expected quantile loss is minimized when following the directive (Gneiting 2011). The quantile scoring function is defined, as in

$$L_{\tau}(z, y) := (z - y) (\mathbb{I}(z \geq y) - \tau), \quad (1)$$

where  $\tau, y$  and  $z$  are the quantile level, the observation and the prediction, respectively, and  $\mathbb{I}(A)$  is the indicator function, which is equal to 1 when the event  $A$  realizes and equal to 0 otherwise. Further information on the quantile scoring function relevant to remote sensing applications can be found in Papacharalampous et al. (2024).

**Table 1.** Individual algorithms used for forming each of the ensemble learners.

Name	Abbreviation	Reference(s)
Quantile regression	QR	Koenker and Bassett (1978); Koenker (2005)
Quantile regression forests	QRF	Meinshausen and Ridgeway (2006)
Generalized random forests	GRF	Athey et al. (2019)
Gradient boosting machines	GBM	Friedman (2001); Mayr et al. (2014)
Light gradient boosting machines	LightGBM	Ke et al. (2017)
Quantile regression neural networks	QRNN	Taylor (2000); Cannon (2011)

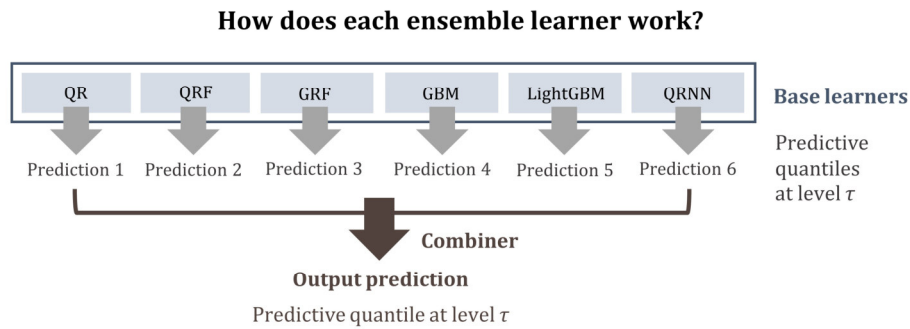
### 2.2 Ensemble learners

Let us suppose that we are interested in predicting the quantile functional at level  $\tau$  by combining the independent predictions of two or more quantile regression algorithms

(base learners). For this case, this paper proposes the utilization of a quantile regression algorithm as the combiner. Under this strategy, the predictions of the base learners for the quantile functional at level  $\tau$  are used as predictor variables for the combiner, with the predictand being the quantile functional at level  $\tau$ . Due to the properties of the quantile regression algorithms (minimization of the quantile scoring function), the strategy introduced is expected to lead to optimal predictions for the quantile functional compared to the base learners (van der Laan 2007; Wolpert 1992; Yao et al. 2018). A pseudo algorithm for the implementation of the ensemble in a training set of  $n$  samples follows:

- Step 1: Split the training set randomly into set 1 with  $n_1$  samples and set 2 with  $n_2$  samples; where  $n_1 + n_2 = n$ .
- Step 2: Train quantile regression algorithms 1, ...,  $k$  in set 1 to predict quantile  $q_\tau$  at level  $\tau$ . Let the predictions of the set 1 trained algorithms in set 2 be notated with  $q_{1,\tau}$  ...,  $q_{k,\tau}$  respectively.
- Step 3: Train the combiner in set 2, using  $q_{1,\tau}$  ...,  $q_{k,\tau}$  as predictors to minimize the quantile average score at level  $\tau$ .
- Step 4: Retrain quantile regression algorithms 1, ...,  $k$  in the full training set (union of set 1 and set 2) to predict quantiles  $q_\tau$  at level  $\tau$ . Let the predictions of the full set trained algorithms in the test set be notated with  $q_{\text{upd},1,\tau}$  ...,  $q_{\text{upd},k,\tau}$  respectively.
- Step 5: Issue quantile predictions in the test set with the trained combiner of step 3 using  $q_{\text{upd},1,\tau}$  ...,  $q_{\text{upd},k,\tau}$  as predictor values.

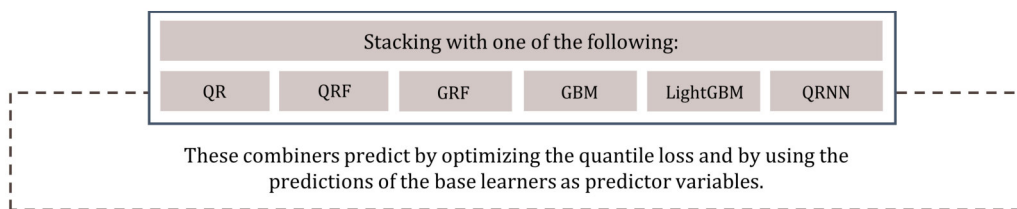
Six stacking methods were formulated based on the above concepts. All of them use the total of the individual quantile regression algorithms in Table 1 as their base learners and each of them uses a different individual quantile regression algorithm as its combiner. The parameters of the individual algorithms are set as in Papacharalampous et al. (2024). To provide benchmarks for these ensemble learners methods (other than the individual quantile regression algorithms in Table 1, which are also reasonable benchmarks), three simple ensemble learners were formulated. Their base learners are the same as for the stacking methods and their combiners are the mean of the predictive quantiles, the median of the predictive quantiles and the best learner. In summary, the ensemble learners are described in Figure 1. In summary 15 algorithms were compared including the six base learners, the six stacking algorithms, the mean, the median and the best learner.



**What is the difference between the ensemble learners?**

They utilize different combiners.

**Which are the combiners introduced in this study?**



**Which are the benchmark combiners?**

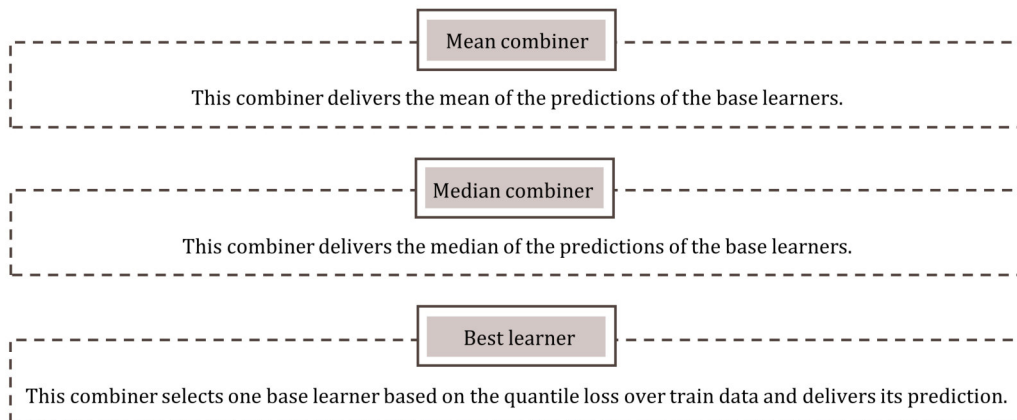


**Figure 1.** Ensemble learners formulated in this study and their combiners. QR, QRF, GRF, GBM, LightGBM and QRNN stand for quantile regression, quantile regression forests, generalized random forests, gradient boosting machines, light gradient boosting machines and quantile regression neural networks, respectively.

**3. Datasets and application**

**3.1 Datasets**

We applied the nine ensemble learners (see [Section 2](#)) and the six individual algorithms (QR, QRF, GRF, GBM, LightGBM and QRNN) for estimating predictive uncertainty while merging remote sensing and gauge-measured data. For this application, data from four

databases were sourced (see [Tables 2–4](#)). The same data were previously exploited all together in different experiments by Papacharalampous et al. (2023c, 2024).

**Table 2.** Databases from which data were retrieved for this study.

Name	Abbreviation	Data type	Reference
Global Historical Climatology Network monthly database, version 2	GHCNm	Gauge-measured precipitation	Peterson and Vose (1997)
Precipitation Estimation from Remotely Sensed Information using Artificial Neural Networks	PERSIANN	Remote sensed precipitation	Hsu et al. (1997); Nguyen et al. (2018); Nguyen et al. (2019)
GPM Integrated Multi-satellitE Retrievals late precipitation L3 1 day 0.1 degree x 0.1 degree V06	IMERG	Remote sensed precipitation	Huffman et al. (2019)
Amazon Web Services Terrain Tiles	AWSTT	Elevation	–

**Table 3.** Sources of databases from which data were retrieved for this study.

Database	Source
GHCNm	National Oceanic and Atmospheric Administration (NOAA)
PERSIANN	Centre for Hydrometeorology and Remote Sensing (CHRS), University of California, Irvine (UCI)
IMERG	National Aeronautics and Space Administration (NASA) Goddard Earth Sciences (GES) Data and Information Services Center (DISC)
AWSTT	Amazon Web Services (AWS)

**Table 4.** Data retrieval details.

Dataset	Address	Date accessed
GHCNm	<a href="https://www.ncei.noaa.gov/pub/data/ghcn/v2">https://www.ncei.noaa.gov/pub/data/ghcn/v2</a>	2022-09-24
PERSIANN	<a href="https://chrsdata.eng.uci.edu">https://chrsdata.eng.uci.edu</a>	2022-03-07
IMERG	<a href="https://doi.org/10.5067/GPM/IMERGD/06">https://doi.org/10.5067/GPM/IMERGD/06</a>	2022-12-10
AWSTT	<a href="https://registry.opendata.aws/terrain-tiles">https://registry.opendata.aws/terrain-tiles</a>	2022-09-25

The precipitation data refer to the years 2001–2015 and to the locations shown in [Figures 2 and 3](#) for the gauge-measured and the remote sensing data, respectively. In particular, 1 421 gauges offered data for this study, while the spatial resolution of both remote sensing datasets is 0.25 degree x 0.25 degree. Bilinear interpolation was applied to the original IMERG dataset for obtaining precipitation at this spatial resolution, as the PERSIANN dataset was available at it. Furthermore, as the PERSIANN and IMERG data originally extracted were daily in opposition to the total monthly data from GHCNm, total monthly PERSIANN and IMERG data had to be formed through time series aggregation. The elevation data refer to the locations shown in [Figure 2](#) (i.e., the locations of the ground-based stations).

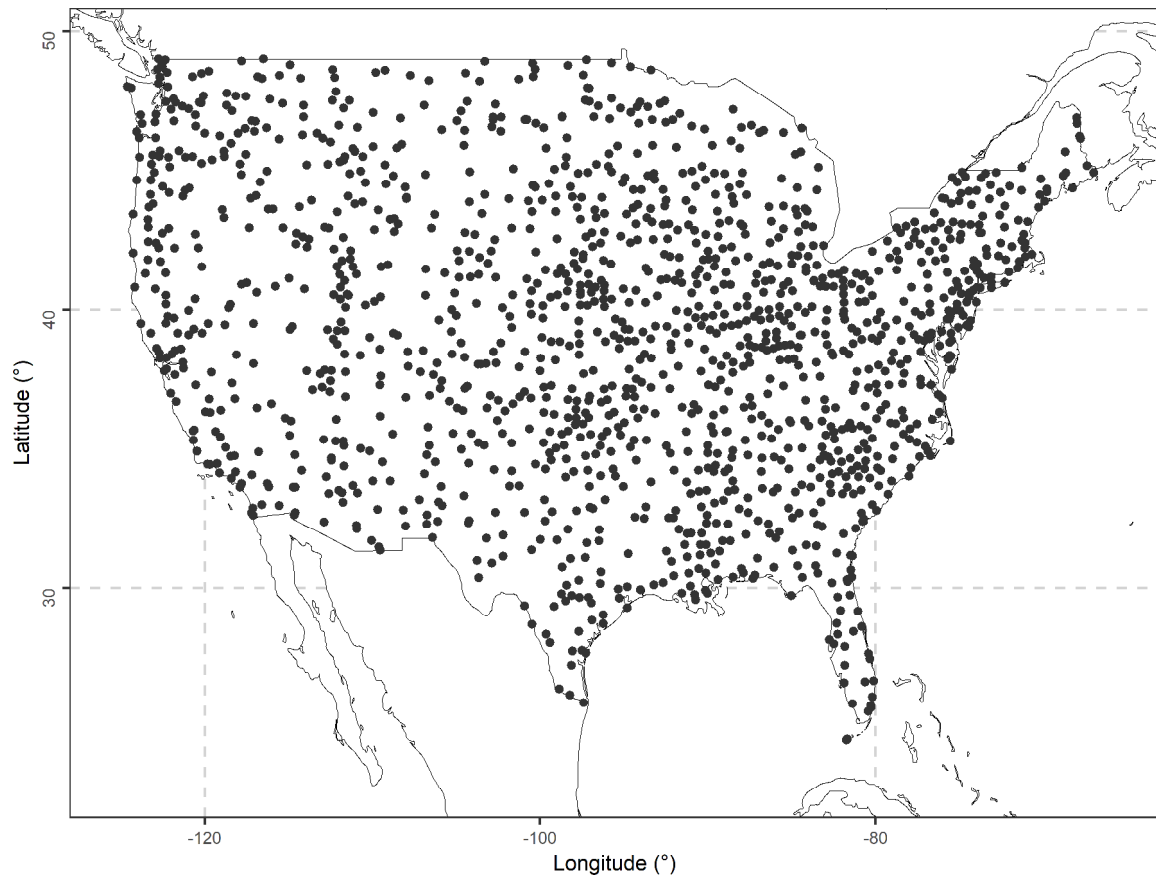


Figure 2. Locations of the ground-based stations that offered time series for this study.

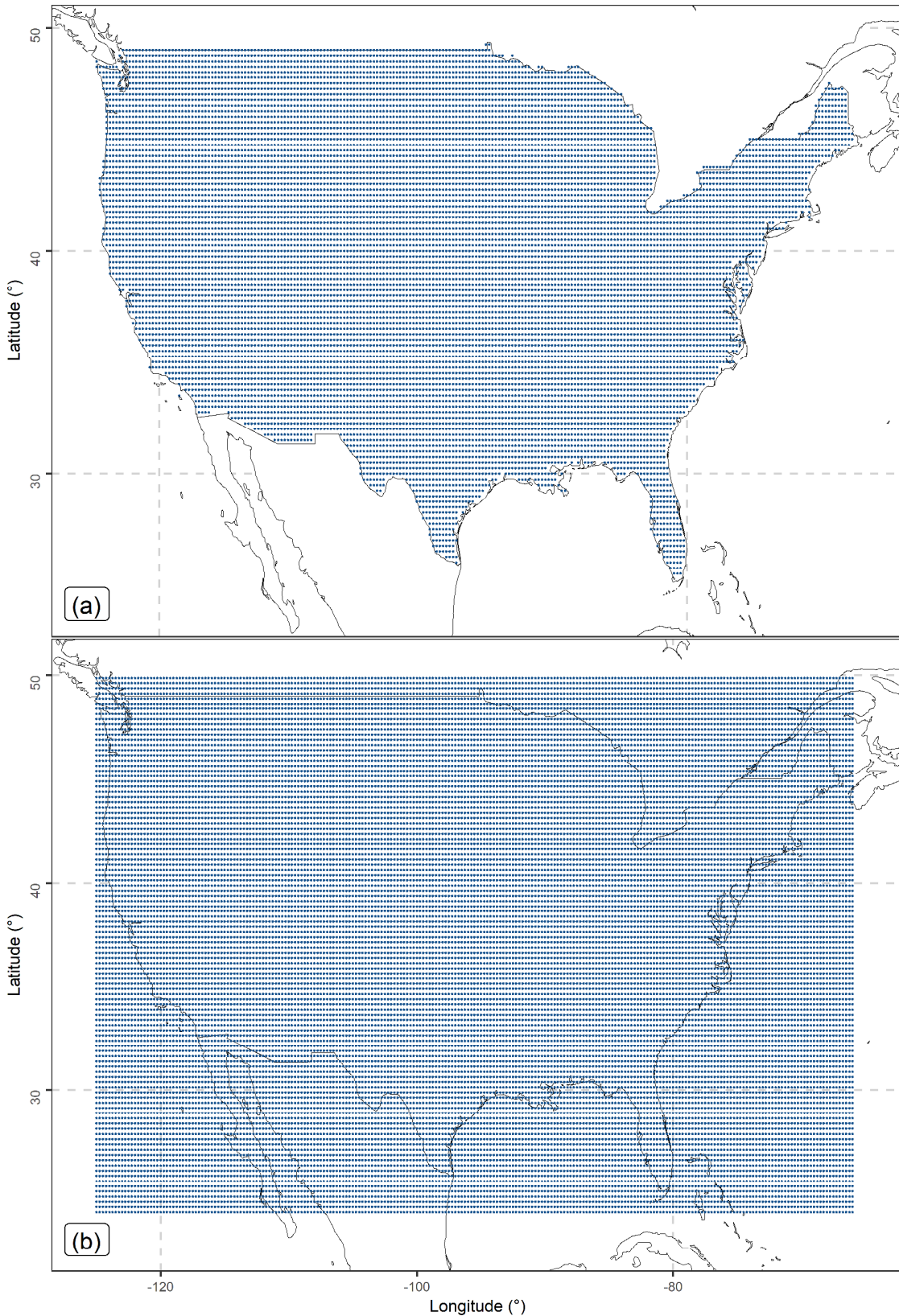


Figure 3. Locations of the grid points with (a) PERSIANN and (b) IMERG data.

### 3.2 Algorithm implementation

The remote sensing data are inaccurate but available at a dense spatial grid. On the other

hand, the gauge-measured data are accurate but available only for the locations shown in [Figure 2](#). To form accurate precipitation data at a dense spatial grid via prediction, we can merge remote sensing and gauge-measured precipitation data using machine learning. To simultaneously assess the predictive uncertainty of the new data and, therefore, provide probabilistic instead of point predictions, we can use machine learning algorithms such as those described in [Section 2](#). For the merging, the remote sensing data can be used as predictor variables, together with topography variables, and the gauge-measured data should take the role of the predictand; because they are the ground-truth. Relevant spatial interpolation settings are available, for instance, in [Baez-Villanueva et al. \(2020\)](#) and [Papacharalampous et al. \(2023b\)](#).

Let the distances of a given station (station 1) from its four closest grid points (grid points 1–4) be denoted with  $d_i$ , where  $i = 1, 2, 3$  and  $4$  ([Figure 4](#)). Herein, these distances and the remote sensing data at the same grid points were used to apply distance-based weighting, separately for each remote sensing dataset. More precisely, the distance-weighted precipitation  $\dot{\text{PR}}_k$  at grid point  $k = 1, \dots, 4$ , is defined, as in

$$\dot{\text{PR}}_k = \frac{(1/d_k^2)\text{PR}_k}{\sum_{i=1}^4 1/d_i^2}, k = 1, \dots, 4, \quad (2)$$

where  $\text{PR}_k$  is the raw satellite precipitation at grid point  $k$ . The variables represented by the distance-based weighted precipitation values are referred to hereinafter as “PERSIANN variables 1–4” and “IMERG variables 1–4”, and are the predictor variables for predicting the precipitation value at station 1, together with the elevation at the same station. Using distance-weighted precipitation allows us to halve the number of predictor variables in a physically principled manner (closer points are assigned higher weights), while simultaneously reducing the redundancy introduced by repeated distance values. However, while the reduced number of variables may contain less information, this is potentially compensated for by the improved performance of non-tree-based algorithms, which can be sensitive to such redundancies.

Satellite data grid	●	Gauge station	●
Distance, $d_i, i = 1, 2, 3, 4$		$d_1 < d_2 < d_3 < d_4$	

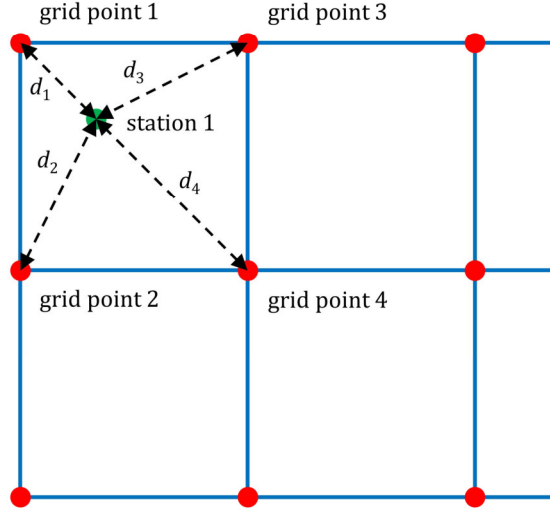


**Figure 4.** Technical details of the application of the algorithms in this study. The remote sensing data are inaccurate but available at all the grid points, while the station-measured data are accurate but available only for the locations shown in Figure 2. Precipitation at the stations is the target variable. The distances of a given station (station 1) from its four closest grid points (grid points 1–4) are denoted with  $d_i, i = 1, 2, 3$  and 4. These distances and the remote sensing precipitation data at the same grid points were used to compute eight predictor variables with distance-based weighting.

The dataset was composed by 91 623 samples, each of which contained 10 values. In particular, a sample is of the form  $\text{sample}_i = \{\text{PR}_{\text{station}}, \dot{\text{P}}\text{R}_{1,\text{IMERG}}, \dot{\text{P}}\text{R}_{2,\text{IMERG}}, \dot{\text{P}}\text{R}_{3,\text{IMERG}}, \dot{\text{P}}\text{R}_{4,\text{IMERG}}, \dot{\text{P}}\text{R}_{1,\text{PERSIANN}}, \dot{\text{P}}\text{R}_{2,\text{PERSIANN}}, \dot{\text{P}}\text{R}_{3,\text{PERSIANN}}, \dot{\text{P}}\text{R}_{4,\text{PERSIANN}}, \text{elevation}_{\text{station}}\}, i = 1, \dots, 91\ 623$ , where  $\text{PR}_{\text{station}}$  is the observed precipitation at a station in a specified month,  $\dot{\text{P}}\text{R}_{k,\text{IMERG}}$  and  $\dot{\text{P}}\text{R}_{k,\text{PERSIANN}}, k = 1, \dots, 4$  are the distance-weighted satellite precipitations in the same month and  $\text{elevation}_{\text{station}}$  is the station’s elevation. In the regression setting,  $\text{PR}_{\text{station}}$  is the dependent variable and the sample’s remaining variables are the predictors.

The dataset was randomly split into three equally-sized sets. The first of these sets was used to train the individual algorithms (which were applied as described in Papacharalampous et al. 2024), and the second for making predictions of the same algorithms. The predictions for the second set were used by the best learner, together with their corresponding true values, for identifying a single best algorithm based on the quantile scoring function averaged across the samples of set 2. They were also used as predictor variables by the stacking algorithms for training the combiners to predict the true values (see the pseudo algorithm in Section 2.2). Then, the individual algorithms were trained on the union of sets 1 and 2, and predictions were obtained for set 3. These

predictions were used for forming the predictions of all the ensemble learners for set 3 (see the pseudo algorithm in [Section 2.2](#)). Additionally, they were used for benchmarking the ensemble learners.

Predictive quantiles at a dense grid consist an approximation of the predictive probability distribution. In this work, predictions were made for the quantile levels  $\tau \in \{0.025, 0.050, 0.075, 0.100, 0.200, 0.300, 0.400, 0.500, 0.600, 0.700, 0.800, 0.900, 0.925, 0.950, 0.975\}$ . As precipitation cannot be negative, negative predictions at the quantile were set to zero. To ensure that predictive quantiles do not cross, for each set {data sample, algorithm}, any prediction that was smaller than the prediction of the immediate lower quantile level was set equal to the latter prediction.

### 3.3 Performance comparison

For each set {predictive  $\tau$ -quantile, algorithm}, a quantile score was computed according to Equation (1) in the test. Then, separately for each algorithm, the quantile scores were averaged over the test dataset, as in

$$\bar{L}_\tau(z, y) := (1/k) \sum_{i=1}^k L_\tau(z_i, y_i), \quad (3)$$

where  $k$  is the number of samples included in the test dataset, and  $y_i$  and  $z_i$ ,  $i \in \{1, \dots, k\}$  are the observation and  $\tau$ -quantile prediction, respectively, of the  $i^{\text{th}}$  sample.

As the average quantile scores, are not scaled, quantile skill scores were computed, as in

$$L_{\tau, \text{skill}} := 1 - \bar{L}_{\tau, \text{algorithm}} / \bar{L}_{\tau, \text{benchmark}}, \quad (4)$$

where the benchmark is QR, which is the simpler algorithm. The quantile skill score takes values between  $-\infty$  and 1. Quantile skill score larger (smaller) than zero indicates that the predictions of the algorithm of interest are better (worse) than the predictions of the benchmark. Quantile skill score equal to 1 indicates that the predictions of the algorithm of interest are perfect. For an easier comparison between the algorithms, their ranking based on the quantile skill score was obtained for each quantile level.

Additionally, frequencies (sample coverages) were computed. More precisely, for each set {algorithm, quantile level} and for the entire dataset, the frequency with which the prediction is smaller or equal to its corresponding observation was computed. The closer the sample coverages to their nominal values, the larger the reliability of the predictions.

### 3.4 Predictor variable importance

GRF and LightGBM were additionally used to investigate predictor variable importance in two settings. In the first one, the predictor variables were the IMERG variables 1–4, the PERSIANN variables 1–4 and the elevation at the station when GRF and LightGBM were trained on the entire data sample. In the second setting, the predictor variables were the predictions by the base learners (QR, QRF, GRF, GBM, LightGBM and QRNN) in the stacked generalization frameworks where GRF and LightGBM are the combiners. For each set {setting, quantile level, predictor variable}, a simple weighted sum of how many times the predictor variable was split on at each depth in the forest was computed through GRF (Tibshirani and Athey 2023), and the total gain in splits (Shi et al. 2023) was computed through LightGBM. These statistics should be interpreted as follows: The larger their values, the larger the importance of the predictor variable. Based on this, ranks of the predictor variables at each quantile level were obtained. The smaller the rank of a predictor variable, the more important this predictor variable.

## 4. Results

### 4.1 Comparison of algorithms

In summary, the algorithms predicted the quantile functional at several levels. Thus, their comparison should rely on a scoring function that is strictly consistent for this functional. Herein, we selected the quantile scoring function. To facilitate comparisons across the entire sample, we computed quantile skill scores. The latter are presented in Figure 5a, while the ranks of the algorithms based on these scores are presented in Figure 5b. For all the quantile levels, stacking with QR and stacking with QRNN are the two best-performing algorithms. For the quantile levels {0.075, 0.100, 0.200, 0.300, 0.400, 0.500, 0.600, 0.700, 0.800}, LightGBM and the best learner exhibit the same performance and share the third position. Other algorithms that exhibit good performance are stacking with GBM from the ensemble learners, and QRF and GBM from the individual algorithms. The mean and median combiners are ranked before QR, GBM and QRNN, but after the remaining individual algorithms. The worst among all the stacking methods, for the problem investigated, is stacking with LightGBM.

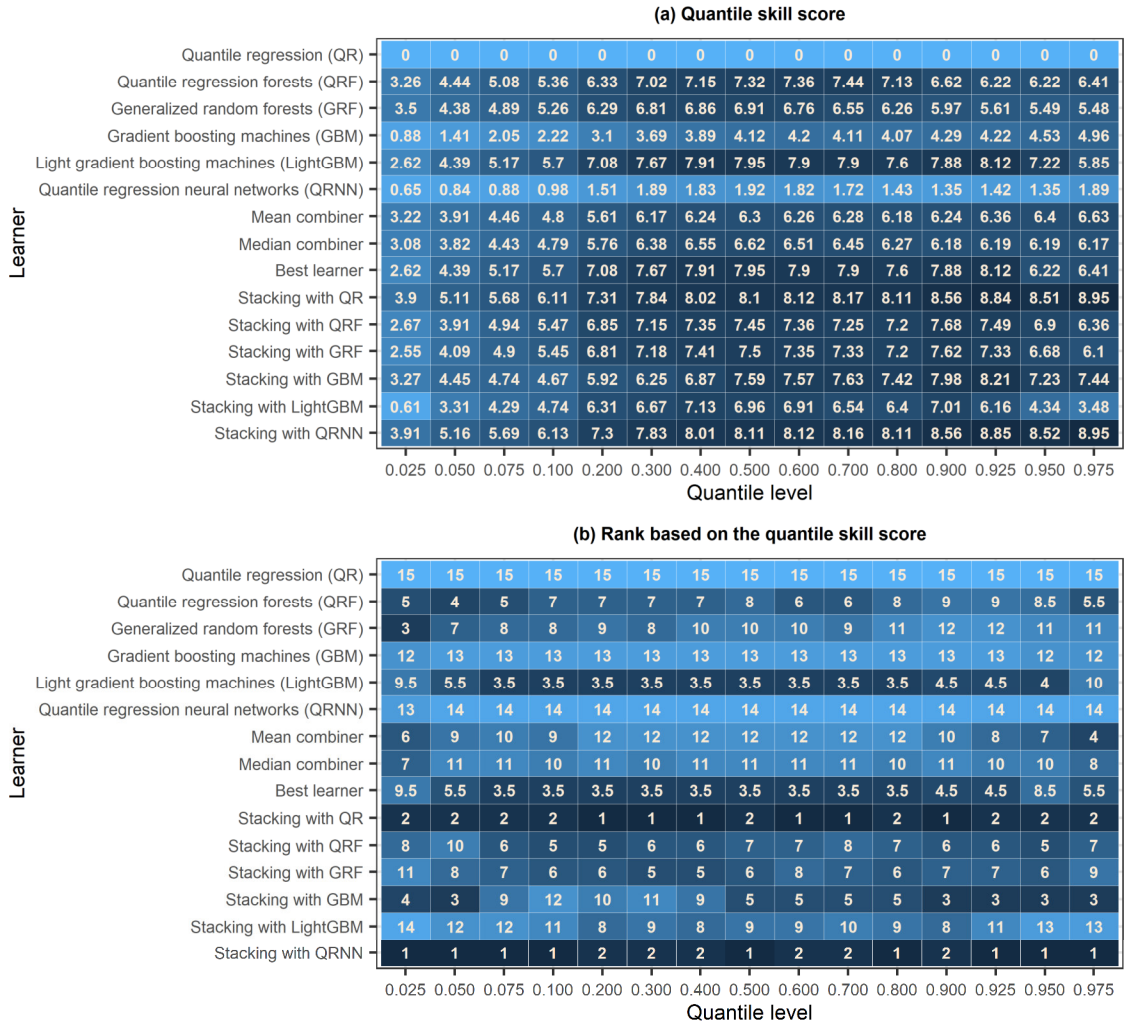


**Figure 5.** (a) Quantile skill score and (b) rank of each of the algorithms at the various quantile levels. The larger the quantile skill score, the smaller the rank and the darker the colour, the better the predictions on average compared to the predictions of quantile regression.

The sample coverages of the quantile predictions at the various quantile levels could also be of interest. [Figure 6](#) shows that these statistics are close to their nominal values for the quantile predictions of all the algorithms. Although, predictive coverages are intuitive and serve to understand whether the predictions are good in an absolute sense, they are not consistent (please recall the definition of consistency of a scoring function in [Section 2.1](#)). To this end, ranking of the algorithms should be based on quantile scoring functions, as presented in [Figure 5](#). Recall from [Section 2.1](#), that are quantile scoring functions are consistent for quantile functionals; therefore they allow honest evaluations of quantile predictions.

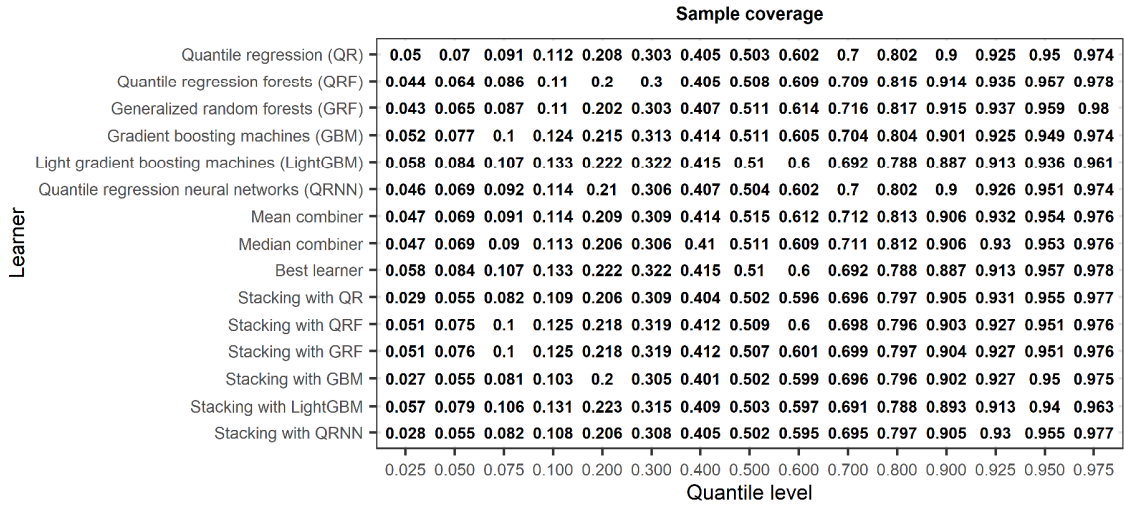


Figure 6. Sample coverage of the predictions of the algorithms at the various quantile levels. The closest the sample coverage to its nominal value (quantile level), the more reliable the predictions on average.

#### 4.2 Importance of base learners in stacking

Figure 7 presents the ranks of the predictions of the base learners at the various quantile levels based on the importance of these predictions as predictors in stacking in the application of interest. According to explainable ML procedures of both the GRF and LightGBM algorithms, the predictions of LightGBM consist the most important predictor, while the predictions of QRF and GRF are also important. These results are in agreement with the ranks of the individual learners based on the quantile skill score (Figure 5b).

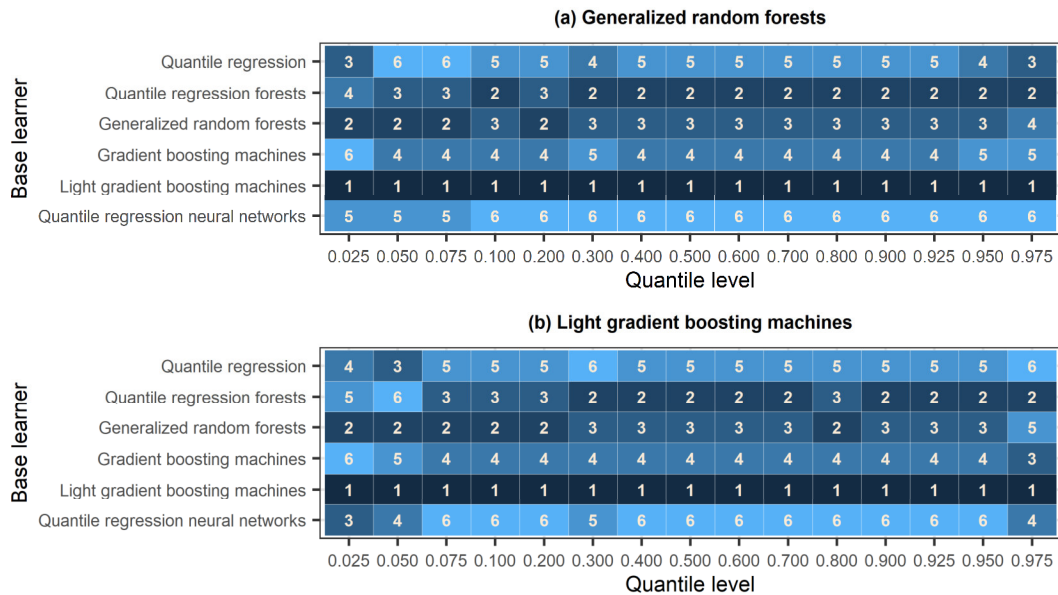


Figure 7. Ranking of the base learners at the various quantile levels based on (a) generalized random forests and (b) light gradient boosting machines. The smaller the rank and the darker the colour, the more useful the predictions of the base learners.

### 4.3 Importance of predictor variables

Figure 8 presents the order at each quantile level of the predictor variables based on their importance in predictive uncertainty estimation in the application of this study. According to explainable ML procedures of both the GRF and LightGBM algorithms, the IMERG product offers more important predictors than the PERSIANN product, overall. Moreover, the station elevation appears in the second, third or fourth position for the quantile levels equal to or larger than 0.300 according to LightGBM. A final remark concerns the distance-based weighting made for producing the observations for the predictor variables. Because of this weighting, there should not be a priori expectations for the relative importance of the IMERG variables 1–4 (PERSIANN variables 1–4) and, indeed, the variable importance results confirm this; in the sense that ordering of IMERG variables is not constant when varying the quantile level. In previous studies (Papacharalampous et al. 2023c; 2024), where unweighted satellite data were used as predictors, the closer grid data were consistently more important compared to more distant ones.

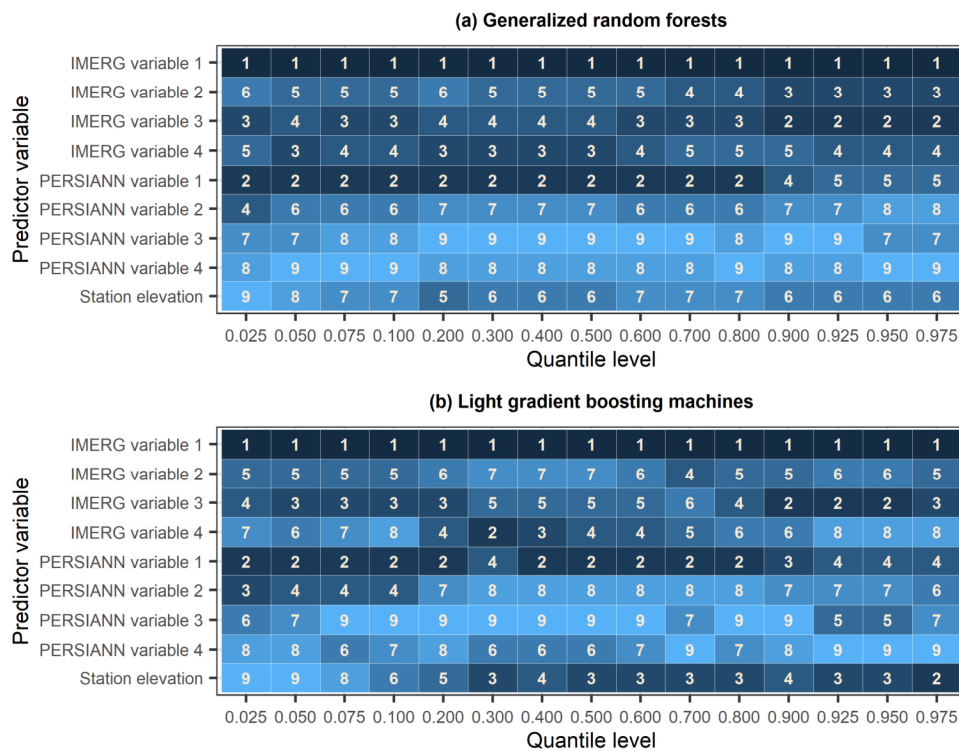


Figure 8. Ranking of the predictors at the various quantile levels based on (a) generalized random forests and (b) light gradient boosting machines. The smaller the rank and the darker the colour, the more important the predictor.

## 5. Discussion

As it is the case for all the categories of machine learning algorithms (Boulesteix et al.

2018), comparisons between ensemble learning methods and comparisons of such methods with individual machine learning algorithms should rely on large datasets. Furthermore, they should include as many algorithms as possible. Complying with these principles, the comparison conducted in this work is of large scale.

Overall, the central methodological contribution of this paper to the machine learning literature concerns the utilization of quantile regression algorithms as combiners in ensemble learning methods for predicting the quantile functional. This new category of combiners can also be used for issuing predictions for the quantile functional through the combination of different machine and statistical learning algorithms (or even physics-based models, Tyralis and Papacharalampous 2021) for predictive uncertainty estimation, even algorithms from families aside from the quantile regression one (see the review by Tyralis and Papacharalampous 2024). On the other hand, for cases in which the interest is in predicting other functionals that are measures of uncertainty as well (such as the expectile functional), algorithms that involve scoring functions which are strictly consistent for these functionals would be reasonable combiners.

Among the nine ensemble learners introduced in this work, stacking of QR, QRF, GRF, GBM, LightGBM and QRNN (base learners) using QR as the combiner and stacking of the same base learners using QRNN as the combiner were proven the best for the problem of predictive uncertainty estimation while merging remote sensing and gauge-measured precipitation data at the monthly time scale. Indeed, the predictions of these ensemble learners scored better than the predictions of the others and the predictions of LightGBM, which is the best individual algorithm for this earth observation and geoinformation task (Papacharalampous et al. 2024). From a theoretical point of view, one could expect that a stacking method outperforms individual algorithms (van der Laan 2007; Wolpert 1992). In this context, the selection of the combiner matters.

In our setting, the simplest combiner (linear QR) performs similarly to QRNN, even though QRNN might be expected to outperform QR. A possible explanation is that the stacking step utilizes a small number of predictor variables (i.e., base learners) and samples, limiting the ability to fully leverage machine learning's power. For example, QRNNs are known to improve generalization with more data. We expect that spatial settings with daily data (almost 30 times larger than monthly datasets) would enable better generalization of machine learning combiners. The relative performance of the nine new ensemble learners might differ in other predictive uncertainty estimation

problems; e.g., when prediction of extremes is of interest (Tyralis and Papacharalampous 2023a; Tyralis et al. 2023). Therefore, all of them, and potentially others, should be evaluated on a problem-by-problem basis to identify optimal machine learning solutions.

## 6. Conclusions

In this study, we formulated six stacking and three simple ensemble learners for predicting quantile functionals. These learners were created by combining six individual quantile regression algorithms in various ways, including novel approaches introduced here for the first time in the machine learning literature. Beyond contributions to this field, the work also offers advancements in applied earth observation and geoinformation. This study presents the first application of ensemble learning to estimate predictive uncertainty while merging remote sensing and gauge-measured data, particularly for precipitation data. Furthermore, we propose a novel feature engineering strategy for merging remote sensing and gauge-measured data. This strategy relies on distance-based weighting of satellite data and halves the number of satellite-based predictor variables with limited loss of information.

The six individual algorithms employed as base learners for all ensemble learners are quantile regression (QR), quantile regression forests, generalized random forests, gradient boosting machines, light gradient boosting machines (LightGBM), and quantile regression neural networks (QRNN). Each of these algorithms was also used to combine the base learners within a stacking framework. Evaluation was based on quantile scores at multiple levels (0.025, 0.050, 0.075, 0.100, 0.200, 0.300, 0.400, 0.500, 0.600, 0.700, 0.800, 0.900, 0.925, 0.950, 0.975) of the predictive probability distribution.

For estimating predictive uncertainty while merging remote sensing and gauge-measured data, stacking using QR and stacking using QRNN achieved the best performance. Compared to the QR reference method, these methods demonstrated improvements ranging from 3.91% to 8.95% depending on the quantile level. LightGBM was the most effective individual base learner in this specific problem, with improvements ranging from 2.62% to 8.12%. However, ensemble learners significantly outperformed LightGBM at higher quantile levels. For example, the QRNN-based stacking method demonstrated an improvement of 8.95% at the 0.975 level compared to a 5.85% improvement for LightGBM. It is important to note that the relative performance of both ensemble and base learners is likely to vary depending on the specific problem and should

be evaluated on a case-by-case basis.

**Conflicts of interest:** There is no conflict of interest.

**Funding:** This work was conducted in the context of the research project BETTER RAIN (BENefiTting from machine LEarning algoRithms and concepts for correcting satellite RAINfall products). This research project was supported by the Hellenic Foundation for Research and Innovation (H.F.R.I.) under the “3<sup>rd</sup> Call for H.F.R.I. Research Projects to support Post-Doctoral Researchers” (Project Number: 7368).

**Acknowledgements:** Currently not applicable.

## Appendix A Statistical software

The R programming language (R Core Team 2024) and the R packages listed in Table A1 were used to program the ensemble learners and conduct the application of this study.

**Table A1.** R packages used for conducting this study and their utilities.

R package	Reference(s)	Utility in this study	
caret	Kuhn (2023)	Data processing or visualization	
data.table	Barrett et al. (2023)		
elevatr	Hollister (2023)		
ncdf4	Pierce (2023)		
rgdal	Bivand et al. (2023)		
sf	Pebesma (2018, 2023)		
spdep	Bivand (2023), Bivand and Wong (2018), Bivand et al. (2013)		
tidyverse	Wickham et al. (2019), Wickham (2023)		
gbm	Greg and GBM Developers (2024)		Individual algorithm implementation
grf	Tibshirani and Athey (2023)		
lightgbm	Shi et al. (2024)		
qrnn	Cannon (2011, 2018, 2023)		
quantreg	Koenker (2023)		
scoringfunctions	Tyralis and Papacharalampous (2023b, 2024)		
devtools	Wickham et al. (2022)	Report production	
knitr	Xie (2014, 2015, 2023)		
rmarkdown	Allaire et al. (2023), Xie et al. (2018, 2020)		

## References

- [1] Abdollahipour A, Ahmadi H, Aminnejad B (2022) A review of downscaling methods of satellite-based precipitation estimates. Earth Science Informatics

- 15(1):1–20. <https://doi.org/10.1007/s12145-021-00669-4>.
- [2] Allaire JJ, Xie Y, Dervieux C, McPherson J, Luraschi J, Ushey K, Atkins A, Wickham H, Cheng J, Chang W, Iannone R (2023) rmarkdown: Dynamic Documents for R. R package version 2.25. <https://CRAN.R-project.org/package=rmarkdown>.
- [3] Athey S, Tibshirani J, Wager S (2019) Generalized random forests. *Annals of Statistics* 47(2):1148–1178. <https://doi.org/10.1214/18-AOS1709>.
- [4] Baez-Villanueva OM, Zambrano-Bigiarini M, Beck HE, McNamara I, Ribbe L, Nauditt A, Birkel C, Verbist K, Giraldo-Osorio JD, Xuan Think N (2020) RF-MEP: A novel random forest method for merging gridded precipitation products and ground-based measurements. *Remote Sensing of Environment* 239:111606. <https://doi.org/10.1016/j.rse.2019.111606>.
- [5] Barrett T, Dowle M, Srinivasan A (2023) data.table: Extension of 'data.frame'. R package version 1.14.10. <https://CRAN.R-project.org/package=data.table>.
- [6] Bhuiyan MAE, Nikolopoulos EI, Anagnostou EN, Quintana-Seguí P, Barella-Ortiz A (2018) A nonparametric statistical technique for combining global precipitation datasets: Development and hydrological evaluation over the Iberian Peninsula. *Hydrology and Earth System Sciences* 22(2):1371–1389. <https://doi.org/10.5194/hess-22-1371-2018>.
- [7] Bivand RS (2023) spdep: Spatial Dependence: Weighting Schemes, Statistics. R package version 1.3-1. <https://CRAN.R-project.org/package=spdep>.
- [8] Bivand RS, Wong DWS (2018) Comparing implementations of global and local indicators of spatial association. *TEST* 27(3):716–748. <https://doi.org/10.1007/s11749-018-0599-x>.
- [9] Bivand RS, Pebesma E, Gómez-Rubio V (2013) *Applied Spatial Data Analysis with R*. Second Edition. Springer New York, NY. <https://doi.org/10.1007/978-1-4614-7618-4>.
- [10] Bivand RS, Keitt T, Rowlingson B (2023) rgdal: Bindings for the 'Geospatial' Data Abstraction Library. R package version 1.6-6. <https://CRAN.R-project.org/package=rgdal>.
- [11] Boulesteix AL, Binder H, Abrahamowicz M, Sauerbrei W (2018) Simulation Panel of the STRATOS Initiative. On the necessity and design of studies comparing statistical methods. *Biometrical Journal* 60(1):216–218. <https://doi.org/10.1002/bimj.201700129>.
- [12] Cannon AJ (2011) Quantile regression neural networks: Implementation in R and application to precipitation downscaling. *Computers and Geosciences* 37(9):1277–1284. <https://doi.org/10.1016/j.cageo.2010.07.005>.
- [13] Cannon AJ (2018) Non-crossing nonlinear regression quantiles by monotone composite quantile regression neural network, with application to rainfall extremes. *Stochastic Environmental Research and Risk Assessment* 32(11):3207–3225. <https://doi.org/10.1007/s00477-018-1573-6>.
- [14] Cannon AJ (2023) qrnn: Quantile Regression Neural Network. R package version 2.1. <https://CRAN.R-project.org/package=qrnn>.
- [15] Efron B, Hastie T (2016) *Computer Age Statistical Inference*. Cambridge University Press, New York. <https://doi.org/10.1017/CB09781316576533>.
- [16] Friedman JH (2001) Greedy function approximation: A gradient boosting machine. *The Annals of Statistics* 29(5):1189–1232. <https://doi.org/10.1214/aos/1013203451>.
- [17] Glawion L, Polz J, Kunstmann HG, Fersch B, Chwala C (2023) spateGAN: Spatio-temporal downscaling of rainfall fields using a cGAN approach.

- <https://doi.org/10.22541/essoar.167690003.33629126/v1>.
- [18] Gneiting T (2011) Making and evaluating point forecasts. *Journal of the American Statistical Association* 106(494):746–762. <https://doi.org/10.1198/jasa.2011.r10138>.
- [19] Gneiting T, Raftery AE (2007) Strictly proper scoring rules, prediction, and estimation. *Journal of the American Statistical Association* 102(477):359–378. <https://doi.org/10.1198/016214506000001437>.
- [20] Greg R, GBM Developers (2024) gbm: Generalized Boosted Regression Models. R package version 2.1.9. <https://CRAN.R-project.org/package=gbm>.
- [21] Hastie T, Tibshirani R, Friedman J (2009) *The Elements of Statistical Learning*. Springer, New York. <https://doi.org/10.1007/978-0-387-84858-7>.
- [22] Hollister JW (2023) elevatr: Access Elevation Data from Various APIs. R package version 0.99.0. <https://CRAN.R-project.org/package=elevatr>.
- [23] Hsu K-L, Gao X, Sorooshian S, Gupta HV (1997) Precipitation estimation from remotely sensed information using artificial neural networks. *Journal of Applied Meteorology* 36(9):1176–1190. [https://doi.org/10.1175/1520-0450\(1997\)036<1176:PEFRSI>2.0.CO;2](https://doi.org/10.1175/1520-0450(1997)036<1176:PEFRSI>2.0.CO;2).
- [24] Hu Q, Li Z, Wang L, Huang Y, Wang Y, Li L (2019) Rainfall spatial estimations: A review from spatial interpolation to multi-source data merging. *Water* 11(3):579. <https://doi.org/10.3390/w11030579>.
- [25] Huffman GJ, Stocker EF, Bolvin DT, Nelkin EJ, Tan J (2019) GPM IMERG Late Precipitation L3 1 day 0.1 degree x 0.1 degree V06, Edited by Andrey Savtchenko, Greenbelt, MD, Goddard Earth Sciences Data and Information Services Center (GES DISC), Accessed: [2022-10-12], <https://doi.org/10.5067/GPM/IMERGDL/DAY/06>.
- [26] James G, Witten D, Hastie T, Tibshirani R (2013) *An Introduction to Statistical Learning*. Springer, New York. <https://doi.org/10.1007/978-1-4614-7138-7>.
- [27] Ke G, Meng Q, Finley T, Wang T, Chen W, Ma W, Ye Q, Liu TY (2017) Lightgbm: A highly efficient gradient boosting decision tree. *Advances in Neural Information Processing Systems* 30:3146–3154.
- [28] Koenker RW (2005) *Quantile regression*. Cambridge University Press, Cambridge, UK.
- [29] Koenker RW (2023) quantreg: Quantile Regression. R package version 5.97. <https://CRAN.R-project.org/package=quantreg>.
- [30] Koenker RW, Bassett Jr G (1978). Regression quantiles. *Econometrica* 46(1):33–50. <https://doi.org/10.2307/1913643>.
- [31] Kuhn M (2023) caret: Classification and Regression Training. R package version 6.0-94. <https://CRAN.R-project.org/package=caret>.
- [32] van der Laan MJ, Polley EC, Hubbard AE (2007) Super Learner. *Statistical Applications in Genetics and Molecular Biology* 6(1). <https://doi.org/10.2202/1544-6115.1309>.
- [33] Lichtendahl Jr KC, Grushka-Cockayne Y, Winkler RL (2013) Is it better to average probabilities or quantiles?. *Management Science* 59(7):1479–1724. <https://doi.org/10.1287/mnsc.1120.1667>.
- [34] Mayr A, Binder H, Gefeller O, Schmid M (2014) The evolution of boosting algorithms: From machine learning to statistical modelling. *Methods of Information in Medicine* 53(6):419–427. <https://doi.org/10.3414/ME13-01-0122>.
- [35] Meinshausen N, Ridgeway G (2006) Quantile regression forests. *Journal of*

- Machine Learning Research 7:983–999.
- [36] Nguyen P, Ombadi M, Sorooshian S, Hsu K, AghaKouchak A, Braithwaite D, Ashouri H, Rose Thorstensen A (2018) The PERSIANN family of global satellite precipitation data: A review and evaluation of products. *Hydrology and Earth System Sciences* 22(11):5801–5816. <https://doi.org/10.5194/hess-22-5801-2018>.
- [37] Nguyen P, Shearer EJ, Tran H, Ombadi M, Hayatbini N, Palacios T, Huynh P, Braithwaite D, Updegraff G, Hsu K, Kuligowski B, Logan WS, Sorooshian S (2019) The CHRS data portal, an easily accessible public repository for PERSIANN global satellite precipitation data. *Scientific Data* 6:180296. <https://doi.org/10.1038/sdata.2018.296>.
- [38] Nguyen GV, Le X-H, Van LN, Jung S, Yeon M, Lee G (2021) Application of random forest algorithm for merging multiple satellite precipitation products across South Korea. *Remote Sensing* 13(20):4033. <https://doi.org/10.3390/rs13204033>.
- [39] Papacharalampous GA, Tyralis H (2022) A review of machine learning concepts and methods for addressing challenges in probabilistic hydrological post-processing and forecasting. *Frontiers in Water* 4:961954. <https://doi.org/10.3389/frwa.2022.961954>.
- [40] Papacharalampous GA, Tyralis H, Doulamis A, Doulamis N (2023a) Comparison of machine learning algorithms for merging gridded satellite and earth-observed precipitation data. *Water* 15(4):634. <https://doi.org/10.3390/w15040634>.
- [41] Papacharalampous GA, Tyralis H, Doulamis A, Doulamis N (2023b) Comparison of tree-based ensemble algorithms for merging satellite and earth-observed precipitation data at the daily time scale. *Hydrology* 10(2):50. <https://doi.org/10.3390/hydrology10020050>.
- [42] Papacharalampous GA, Tyralis H, Doulamis N, Doulamis A (2023c) Ensemble learning for blending gridded satellite and gauge-measured precipitation data. *Remote Sensing* 15(20):4912. <https://doi.org/10.3390/rs15204912>.
- [43] Papacharalampous GA, Tyralis H, Doulamis N, Doulamis A (2024) Uncertainty estimation in satellite precipitation interpolation with machine learning. <https://arxiv.org/abs/2311.07511>.
- [44] Pebesma E (2018) Simple features for R: Standardized support for spatial vector data. *The R Journal* 10(1):439–446. <https://doi.org/10.32614/RJ-2018-009>.
- [45] Pebesma E (2023) sf: Simple Features for R. R package version 1.0-15. <https://CRAN.R-project.org/package=sf>.
- [46] Peterson TC, Vose RS (1997) An overview of the Global Historical Climatology Network temperature database. *Bulletin of the American Meteorological Society* 78(12):2837–2849. [https://doi.org/10.1175/1520-0477\(1997\)078<2837:A00TGH>2.0.CO;2](https://doi.org/10.1175/1520-0477(1997)078<2837:A00TGH>2.0.CO;2).
- [47] Petropoulos F, Svetunkov I (2020) A simple combination of univariate models. *International Journal of Forecasting* 36(1):110–115. <https://doi.org/10.1016/j.ijforecast.2019.01.006>.
- [48] Pierce D (2023) ncd4: Interface to Unidata netCDF (Version 4 or Earlier) Format Data Files. R package version 1.22. <https://CRAN.R-project.org/package=ncdf4>.
- [49] R Core Team (2024) R: A language and environment for statistical computing. R Foundation for Statistical Computing, Vienna, Austria. <https://www.r-project.org>.
- [50] Sagi O, Rokach L (2018) Ensemble learning: A survey. Wiley Interdisciplinary

- Reviews: Data Mining and Knowledge Discovery 8(4):e1249. <https://doi.org/10.1002/widm.1249>.
- [51] Shi Y, Ke G, Soukhavong D, Lamb J, Meng Q, Finley T, Wang T, Chen W, Ma W, Ye Q, Liu T-Y, Titov N. (2024) lightgbm: Light Gradient Boosting Machine. R package version 4.3.0. <https://CRAN.R-project.org/package=lightgbm>.
- [52] Smith J, Wallis KF (2009) A simple explanation of the forecast combination puzzle. Oxford Bulletin of Economics and Statistics 71(3):331–355. <https://doi.org/10.1111/j.1468-0084.2008.00541.x>.
- [53] Taylor JW (2000) A quantile regression neural network approach to estimating the conditional density of multiperiod returns. Journal of Forecasting 19(4):299–311. [https://doi.org/10.1002/1099-131X\(200007\)19:4<299::AID-FOR775>3.0.CO;2-V](https://doi.org/10.1002/1099-131X(200007)19:4<299::AID-FOR775>3.0.CO;2-V).
- [54] Tibshirani J, Athey S (2023) grf: Generalized Random Forests. R package version 2.3.1. <https://cran.r-project.org/package=grf>.
- [55] Tyralis H, Papacharalampous GA (2021) Quantile-based hydrological modelling. Water 13(23):3420. <https://doi.org/10.3390/w13233420>.
- [56] Tyralis H, Papacharalampous GA (2023a) Hydrological post-processing for predicting extreme quantiles. Journal of Hydrology 617(Part C):129082. <https://doi.org/10.1016/j.jhydrol.2023.129082>.
- [57] Tyralis H, Papacharalampous G (2023b) scoringfunctions: A Collection of Scoring Functions for Assessing Point Forecasts. R package version 0.0.6. <https://CRAN.R-project.org/package=scoringfunctions>.
- [58] Tyralis H, Papacharalampous G (2024) A review of predictive uncertainty estimation with machine learning. Artificial Intelligence Review. <https://doi.org/10.1007/s10462-023-10698-8>.
- [59] Tyralis H, Papacharalampous GA, Doulamis N, Doulamis A (2023) Merging satellite and gauge-measured precipitation using LightGBM with an emphasis on extreme quantiles. IEEE Journal of Selected Topics in Applied Earth Observations and Remote Sensing 16:6969–6979. <https://doi.org/10.1109/JSTARS.2023.3297013>.
- [60] Wang X, Hyndman RJ, Li F, Kang Y (2023) Forecast combinations: An over 50-year review. International Journal of Forecasting 39(3):1518–1547. <https://doi.org/10.1016/j.ijforecast.2022.11.005>.
- [61] Wickham H (2023) tidyverse: Easily Install and Load the 'Tidyverse'. R package version 2.0.0. <https://CRAN.R-project.org/package=tidyverse>.
- [62] Wickham H, Averick M, Bryan J, Chang W, McGowan LD, François R, Golemund G, Hayes A, Henry L, Hester J, Kuhn M, Pedersen TL, Miller E, Bache SM, Müller K, Ooms J, Robinson D, Paige Seidel DP, Spinu V, Takahashi K, Vaughan D, Wilke C, Woo K, Yutani H (2019) Welcome to the tidyverse. Journal of Open Source Software 4(43):1686. <https://doi.org/10.21105/joss.01686>.
- [63] Wickham H, Hester J, Chang W, Bryan J (2022) devtools: Tools to Make Developing R Packages Easier. R package version 2.4.5. <https://CRAN.R-project.org/package=devtools>.
- [64] Wolpert DH (1992) Stacked generalization. Neural Networks 5(2):241–259. [https://doi.org/10.1016/S0893-6080\(05\)80023-1](https://doi.org/10.1016/S0893-6080(05)80023-1).
- [65] Xie Y (2014) knitr: A Comprehensive Tool for Reproducible Research in R. In: Stodden V, Leisch F, Peng RD (Eds) Implementing Reproducible Computational Research. Chapman and Hall/CRC.
- [66] Xie Y (2015) Dynamic Documents with R and knitr, 2nd edition. Chapman and

- Hall/CRC.
- [67] Xie Y (2023) knitr: A General-Purpose Package for Dynamic Report Generation in R. R package version 1.45. <https://CRAN.R-project.org/package=knitr>.
  - [68] Xie Y, Allaire JJ, Golemund G (2018) R Markdown: The Definitive Guide. Chapman and Hall/CRC. ISBN 9781138359338. <https://bookdown.org/yihui/rmarkdown>.
  - [69] Xie Y, Dervieux C, Riederer E (2020) R Markdown Cookbook. Chapman and Hall/CRC. ISBN 9780367563837. <https://bookdown.org/yihui/rmarkdown-cookbook>.
  - [70] Yao Y, Vehtari A, Simpson D, Gelman A (2018) Using stacking to average Bayesian predictive distributions. *Bayesian Analysis* 13(3):917–1003. <https://doi.org/10.1214/17-BA1091>.
  - [71] Zhang Y, Ye A, Nguyen P, Analui B, Sorooshian S, Hsu K (2022) QRF4P-NRT: Probabilistic post-processing of near-real-time satellite precipitation estimates using quantile regression forests. *Water Resources Research* 58(5):e2022WR032117. <https://doi.org/10.1029/2022WR032117>.